Dynamic structure of electrons in Al metal studied by inelastic x-ray scattering

W. Schülke, H. Schulte-Schrepping, and J. R. Schmitz
Institute of Physics, University of Dortmund, D-4600 Dortmund 50, Germany
(Received 13 November 1992)

The dynamic structure factor $S(\mathbf{q},\omega)$ of electrons in single-crystal Al metal was measured with 1.4-eV resolution by means of inelastic x-ray-scattering spectroscopy for $\mathbf{q}$ parallel to [100] and for $\mathbf{q}$ parallel to [110] with $0.37 < q < 2.06$ a.u. using synchrotron radiation from DORIS storage ring. The overall shape of the experimental dynamic structure factors is in agreement with jellium calculations which extend the random-phase approximation by taking into account both local-field corrections and the influence of the momentum-dependent lifetime of the quasiparticles. Besides some $\mathbf{q}$-orientation-dependent fine structure, the $S(\mathbf{q},\omega)$ spectra for $q > 1.1$ a.u. exhibit a $\mathbf{q}$-orientation-independent double-peak or one-peak–one-shoulder fine structure. Whereas the $\mathbf{q}$-orientation-dependent fine structure can be attributed to ion-lattice-induced indentations in the electron-hole excitation continuum due to Bragg reflections, the origin of the $\mathbf{q}$-orientation-independent fine structure could not be clarified definitively. The most probable explanation of this fine structure which is based on semiquantitative agreement with model calculations is the shifting down of unoccupied d-like bands due to the lack of d core-state orthogonalization. Alternative interpretations on the basis of special features of the short-range electron correlations (lifetime effects, multiple-pair excitation, plasmaron ground state) have either failed or have been left on the level of qualitative and somewhat speculative arguments.

I. INTRODUCTION

Important many-particle properties of valence electrons in simple metals are represented by the so-called dynamic structure factor $S(\mathbf{q},\omega)$, which is the Fourier transform in space and time of the ground-state expectation value of the time-dependent density-density correlation operator. Within the limits of the jellium model, treated in the random-phase approximation (RPA), $S(\mathbf{q},\omega)$ can easily be calculated by using the analytical Lindhard-Mermin dielectric function.[1] This way, the ω dependence of $S(\mathbf{q},\omega)$ for $q < q_c$ (q_c is the plasmon cutoff wave vector) is represented by a narrow δ-function-like peak, indicating the excitation of a plasmon. Electron-hole excitations are very strongly damped in this region of momentum transfer q. For $q > q_c$, the dynamic structure factor is determined exclusively by electron-hole excitation, so that $S(\mathbf{q},\omega)$ is a continuous single peaked function of ω, the width of which increases with q. The q dependence of the peak position on the ω scale roughly follows a quadratic dispersion relation for $q < q_c$, levels off within an intermediate range of q ($q_c < q < 2q_c$), and comes back to a quadratic dispersion for $q > 2q_c$, but with a less steep rise.[2] In what follows, we will use this simple jellium-RPA picture as a reference, which enables us to estimate the strength of band-structure and exchange-correlation effects.

Measurements of $S(\mathbf{q},\omega)$ on simple metals performed within the range $q < q_c$ by means of electron-energy-loss spectroscopy (EELS) (see Refs. 3 and 4 for reviews) and inelastic x-ray-scattering spectroscopy (IXSS),[5–7] exhibit some remarkable deviations from the jellium-RPA calculations with regard to peak position and dispersion, as well as with regard to the finite width of the plasmon resonances. These deviations are partly due to the interaction between electrons and the ion lattice (the solid-state band structure), which enables interband transitions and contributes to the finite plasmon width even for $q \approx 0$.[8] The adequate theoretical treatment of band-structure effects needs the calculation of the full dielectric matrix.[9] Another source for the deviations from the above-mentioned jellium-RPA picture are local-field effects (inclusion of exchange and correlation), which can lead to a negative plasmon dispersion,[4] as found for the low-electron-density alkali metal Cs.[10] Furthermore, the core polarization can cause an appreciable peak shift[11] where the treatment of the charge fluctuations of valence and core electrons should be on an equal footing.[12] Finally, it has been demonstrated both theoretically[13,14] and experimentally[15–18] that indentations in the electron-hole excitation continuum due to energy gaps at the zone boundaries can, in special cases, lead to additional collective excitations, the so-called zone-boundary collective states (ZBCS).

Much stronger deviations from the simple jellium-RPA calculations have been found in measurements performed by means of IXSS of the ω dependence of $S(\mathbf{q},\omega)$ for $q > q_c$ on simple metals. Also in this case, these deviations could partly be explained by going beyond RPA (local-field corrections) and taking into account lattice effects on the basis of pseudopotential schemes or effective masses. Thus in the case of Li (Ref. 7) and Be metals,[19] the overall shape of the measured $S(\mathbf{q},\omega)$ curves and their peak position were found to be in rather good agreement with jellium calculations, when these calculations allowed for both (static) local-field[20] and momentum-dependent lifetime[21] corrections and a density-of-states effective mass (Be).[22] Furthermore, some features (dips) of the $\mathbf{q}$-orientation-dependent fine structure in the measured spectra could be attributed to

lattice-induced indentations in the electron-hole excitation continuum due to Bragg reflection. Nevertheless, there exists a fine structure (double-peak or one-peak–one-shoulder) in the measured spectra of Li and Be, which might sometimes be superimposed by lattice-induced effects but can clearly be seen in the polycrystalline spectra, so that it can be assumed to be more or less **q** orientation independent. This type of structure has already been found in early low-resolution IXSS measurements of $S(\mathbf{q},\omega)$ on Li,[6,23] Be,[5,24] and Al,[25] and has been interpreted by Platzman and Eisenberger[25] as a universal property of the strongly correlated electron liquid, especially since the dip position has been found roughly at the same energy position when scaling the energy transfer to the Fermi energy.

These experimental findings have triggered a great deal of theoretical work dedicated to reproducing this **q**-orientation-independent fine structure. These theoretical studies can roughly be divided into two groups.

One group[26–28] holds that quasiparticle lifetime effects in the electron-hole response function constitute the dominant mechanism responsible for that fine structure. They argue that the electron's linewidth is suddenly broadened when the electron has enough excess energy to excite a real plasmon. The broadening gives rise to a corresponding broadened high-frequency part of $S(\mathbf{q},\omega)$ which is contrasted with a much less broadened low-frequency section. At the interface of these two sections, the observed fine structure arises. A number of objections have been made against this quasiparticle lifetime interpretation. The violation of particle conservation has been stressed by several authors.[29,30] Moreover, it has been shown[17] that, within the limits of the quasiparticle lifetime schemes, the calculated fine structure will completely disappear if one uses more realistic models for calculating the inverse lifetime via the self-energy rather than simple step models.[29] But probably the most fundamental objection against the above-mentioned lifetime interpretation has been put forward in Refs. 31–33, on the grounds that the self-energy correction to single-particle propagation within an excited electron-hole pair is forced by these schemes to lie *on* the (single-particle) energy shell. It is clearly demonstrated in Refs. 33 and 34 that, by taking into account off-shell contributions to the self-energy correction, the fine structure of the on-shell lifetime model will disappear.

Another group of authors[31,34–36] have applied diagrammatic perturbation methods to this problem based on a microscopic formulation of Baym and Kadanoff,[37] in which the conservation laws and the frequency-moment sum rules are exactly satisfied. These studies have pointed to the importance of direct, dynamical scattering between particle pairs excited out of the Fermi sea. Also, these authors have found some fine structure in $S(\mathbf{q},\omega)$ at metallic densities, but in most cases with more than two peaks, whose positions were strongly dependent on the momentum transfer q. It has been clearly pointed out by Green *et al.*[38] that it is multiple-pair excitation which alone is responsible for this fine structure. But attempts to find agreement between this type of fine structure and experimental findings have failed.[7]

We should also mention that there have been attempts to explain even the more or less **q**-orientation-independent fine structure in terms of band-structure effects,[19] by looking for excitation gaps which should leave indications behind in $S(\mathbf{q},\omega)$ for a large variety of **q** directions.

All things considered, the search for a better physical understanding of the **q**-orientation-independent fine structure of $S(\mathbf{q},\omega)$ of simple metals and semiconductors remains still quite unsatisfactory.

Therefore, we decided to investigate $S(\mathbf{q},\omega)$ of a simple metal, which can be assumed to be more free-electron-like than Li and Be metals studied so far. We have chosen Al, since its pseudopotential coefficients, which fit the Fermi surface topology well, are much smaller than in the case of Li and Be, so that we could assume less confusion by band structure effects than with Li and Be.

The rest of the paper is organized as follows. In Sec. II, some basic relations are summarized inasmuch as they provide the basis for our model calculations. Section III describes briefly the experimental setup at the DORIS storage ring. In Sec. IV, the results of the measurements on Al single crystals are presented, interpreted both by employing the pseudopotential model calculation, which includes appropriate local-field corrections, and by using semiquantitative arguments based on many-body free-electron calculations of the spectral density function, which take into account the hole-plasmon (plasmaron) coupling.[39] Finally in Sec. V, conclusions are drawn from the comparison of experiment with calculations.

II. BASIC RELATIONS

Inelastic x-ray-scattering spectroscopy (IXSS) means measuring the energy distribution of x rays scattered into a solid angle element $d\Omega$. Thus we obtain relative values of the double differential scattering cross section (DDSCS) $d^2\sigma/d\Omega\, d\omega_2$, which is, within the limits of a first-order perturbation treatment,[40] directly connected with the dynamic structure factor $S(\mathbf{q},\omega)$ of the scattering electron system via

$$d^2\sigma/d\Omega\, d\omega_2=(\mathbf{e}_1\cdot\mathbf{e}_2)^2 r_0^2(\omega_2/\omega_1)S(\mathbf{q},\omega)\ , \tag{1}$$

where ω_1 and ω_2 are the frequencies, $\mathbf{e}_1$ and $\mathbf{e}_2$ are the polarization vectors, and $\mathbf{K}_1$ and $\mathbf{K}_2$ are the wave vectors of the incident and the scattered x-ray photons, respectively. r_0 is the classical electron radius, and **q** is the transferred momentum,

$$\mathbf{q}=\mathbf{K}_1-\mathbf{K}_2,\quad q\approx 2K_1\sin(\theta/2)\ , \tag{2}$$

where θ is the scattering angle. The dynamic structure factor $S(\mathbf{q},\omega)$ is related to the dielectric response function $\varepsilon^{-1}(\mathbf{q},\omega)$ by the so-called fluctuation-dissipation theorem:[41]

$$S(\mathbf{q},\omega)=-(\hbar q^2/4\pi^2e^2n)\,\mathrm{Im}\varepsilon^{-1}(\mathbf{q},\omega)\ . \tag{3}$$

n is the electron density. Neglecting all crystal local-field effects, the response function $\varepsilon^{-1}(\mathbf{q},\omega)$ is simply the reciprocal of the dielectric function $\varepsilon(\mathbf{q},\omega)$. Within the limits of the self-consistent-field theory[42] (which is equivalent to the RPA of a free-electron gas), the dielec-

tric function $\varepsilon(\mathbf{q},\omega)$ is determined by one-electron Bloch states represented by the reduced wave vector $\mathbf{k}$, the band index l, the energy $E(\mathbf{k},l)$, and the Fermi function $f_0(\mathbf{k},l)$ as follows:

$$\varepsilon_{SC}(\mathbf{q},\omega)=1+\lim_{\eta\to 0}\sum_{\substack{\mathbf{k},l\\ \mathbf{k}',l'}}\frac{|\langle \mathbf{k}'l'|\exp(i\mathbf{q}\cdot\mathbf{r})|kl\rangle|^2\{f_0(\mathbf{k}',l')-f_0(\mathbf{k},l)\}}{\hbar\omega+E(\mathbf{k},l)-E(\mathbf{k}',l')+i\eta}\ . \tag{4}$$

Thus $\mathrm{Im}\varepsilon_{SC}(\mathbf{q},\omega)$ and, according to Eq. (3), also $S(\mathbf{q},\omega)$ for $q>q_c$ are governed by the joint density of states:

$$\sum[f_0(\mathbf{k}',l')-f_0(\mathbf{k},l)]\delta[\hbar\omega+E(\mathbf{k},l)-E(\mathbf{k}',l')]\ , \tag{5}$$

where, for a given value of $\hbar\omega$, states on two planes in the extended-zone scheme, perpendicular to $\mathbf{q}$ and separated by q, are combined. Therefore, if an energy gap-"producing" Bragg plane perpendicular to $\mathbf{q}$ is involved, one can expect a dip structure in $\mathrm{Im}\varepsilon_{SC}(\mathbf{q},\omega)$. The way this dip influences $S(\mathbf{q},\omega)$ depends on the value of $\mathbf{q}$. For $q\lesssim q_c$, this dip can produce an additional zero of $\mathrm{Re}\varepsilon_{SC}(\mathbf{q},\omega)$, thus giving rise to an additional collective excitation, the so-called zone-boundary collective state.[13] For larger q, the dip of $\mathrm{Im}\varepsilon_{SC}(\mathbf{q},\omega)$ is reproduced in $S(\mathbf{q},\omega)$, more or less unchanged. One can easily verify that, according to the nearly free-electron approximation, the dispersion of the dip position on the energy-loss scale, $\omega(q)$, should follow the dispersion relation

$$\omega(q)=\hbar q(g-q)/2m\ , \tag{6}$$

where it is assumed that the energy gap belongs to the gth Bragg plane in the unoccupied $\mathbf{k}$ space of the extended-zone scheme ($\mathbf{g}$ is the reciprocal-lattice vector).

Exchange and correlation can be introduced into the calculation of $S(\mathbf{q},\omega)$ by utilizing the static approximation $G(\mathbf{q})$ of the local-field factor $G(\mathbf{q},\omega)$ in

$$\varepsilon(\mathbf{q},\omega)=1+[\varepsilon_{SC}(\mathbf{q},\omega)-1]/\{1-G(\mathbf{q},\omega)[\varepsilon_{SC}(\mathbf{q},\omega)-1]\} \tag{7}$$

first introduced by Hubbard.[43] Following Rahman and Vignale,[28] we can take into account the finite lifetime of electron-hole excitations, as represented in Eq. (4), by adding

$$i[\Gamma(\mathbf{k}',l')+\Gamma(\mathbf{k},l)] \tag{8}$$

to the nominator of Eq. (4), where

$$\Gamma(\mathbf{k},l)=\Gamma(p)=|\mathrm{Im}\Sigma(p)|,\quad p=(2mE(\mathbf{k},l))^{1/2} \tag{9}$$

is the modulus of the imaginary part of the "on-shell approximation" of the self-energy, as can be calculated using a scheme first proposed by Quinn and Terrell.[21] It has already been pointed out in Sec. I that this procedure of introducing self-energy corrections has been criticized in Refs. 31–33. As shown by Ng and Dabrowski,[33] a full account of self-energy effects including off-shell contributions can be obtained via the spectral weight function $A(\mathbf{p},E)$:

$$\mathrm{Im}\epsilon^{-1}(\mathbf{q},\omega)=-(2e^2/4\pi^3\hbar q^2)\int_{-\hbar\omega}^{0}dE\int d\mathbf{p}\ A(\mathbf{p},E)A(\mathbf{p}+\mathbf{q},E+\hbar\omega)\ . \tag{10}$$

We will use this relation in Sec. V for some semiquantitative arguments.

III. EXPERIMENTAL SETUP

The measurements of the DDSCS was performed at the Hamburger Synchrotronstrahlungslabor (HASYLAB) using synchrotron x rays from the storage ring DORIS, where two different experimental setups are utilized. One, described in detail elsewhere,[44] is served by radiation from a bending magnet and consists in a Ge(311) double crystal monochromator and a Si(444) spherically bent crystal analyzer in nearly back reflection geometry (Bragg angle 86.2°). By utilizing dispersion compensation,[45] a 1.4-eV overall energy resolution could be obtained with useful 2.3×10^{10} photons s^{-1} of 7.99 keV at the scattering sample, with the DORIS storage ring operated at 3.7 GeV and 50 mA. The effective diameter $D=4$ cm of the spherically bent analyzer, together with the sample-to-analyzer distance of 80 cm, defines an error $\Delta q=\pm0.05$ a.u. for the momentum transfer, nearly independent of the scattering angle within the range used. (Here, and in what follows, a.u. means atomic units: $\hbar=e=m=1$.)

The other setup[46] employs the radiation of the HARWI ("Harter Röntgen Wiggler"), where the major part of the horizontal divergence of the wiggler is accepted by the first water-cooled plane Si(511) crystal and then sagittally focused to 8-mm horizontal width on to the scattering sample by the second cylindrically bent Si(511) monochromator crystal, which was segmented in order to prevent anticlastic bending.[47] The flux of useful 13.7-keV photons at the sample position was 3.8×10^{12} s^{-1}, with the DORIS storage ring operated at 3.7 GeV and 60 mA. The energy analysis has been done by means of a Si(12 0 0) spherically bent crystal working at a Bragg angle of 86°. Thus an overall energy resolution of 1.6 eV could be obtained. The effective diameter $D=4$ cm of the analyzer crystal and the sample-to-analyzer distance defines an error $\Delta q=0.04$ a.u. of the momentum transfer.

At both setups, the spectral analysis of the scattered radiation was performed by holding the Bragg angle of the analyzer fixed and by varying the primary energy (inverse geometry). The cylindrical sample crystals with 1 cm diameter and 2 mm height have been grown from 99.999 high purity Al and were investigated in reflection

geometry,[48] so that the scattering vector **q** was parallel to [100] and [110], respectively. The Al data were processed as described in detail in Ref. 7. In the first instance, the count rate of the detector at the exit slit of the analyzer is related to the count rate of a detector monitoring the beam leaving the double-crystal monochromator, thus allowing for the variation of the storage ring current. This way, only relative values of the DDSCS are available. They were brought to an absolute scale by utilizing the f-sum rule, as shown in Ref. 7. But this procedure is only applicable as long as the valence-electron part of $S(\mathbf{q},\omega)$ is well separated from the core-electron part, which, for the case of Al, starts at $\hbar\omega = 73$ eV (Al $L_{II,III}$ edge). Therefore absolute scaling was only possible for $q \leq 1.45$ a.u. For larger q, the maxima of the spectra were scaled to the peaks of the corresponding jellium-RPA-calculated $S(\mathbf{q},\omega)$'s. Between 1×10^3 and 2×10^3, counts were collected in each channel around the maxima of the spectra. In order to illustrate the main features of the fine structure, the spectra were smoothed by means of cubic splines, where the algorithm used[49] additionally provides the first three derivatives. In Fig. 1, the result of smoothing a Al **q** parallel to [100] spectrum is demonstrated.

IV. DISCUSSION OF THE RESULTS

A. Survey of the experimental results

In Figs. 2 and 3, measured $S(\mathbf{q},\omega)$ spectra of Al for **q** parallel to [100] and **q** parallel to [110], respectively, both within a range of $0.37 < q < 2.06$ a.u., are presented, smoothed by means of cubic splines. For $q < q_c$ ($q_c \approx 0.7$ a.u.) sharp plasmon resonances are visible, whose width increases with q. The smallest full width at half maximum (FWHM) measured for **q** parallel to [110], $q = 0.37$ a.u., was 2.0 eV, not far from the total resolution of 1.4 eV, so that a plasmon linewidth of 1.4 eV can be deduced, in rather good agreement with corresponding EELS measurements.[50] For $q > q_c$, the experimental dynamic structure factors exhibit a broad spectral distribution with some fine structure on it. Independent of the orientation of **q**, a one-peak–one-shoulder fine structure can be seen for $1.24 < q < 1.66$ a.u. (indicated by arrows), with a dip position around 35 eV. The one-peak–one-shoulder structure merges into a double-peak structure for $1.86 < q < 2.06$ a.u. The dip position of both types of fine structure, defined by zeros of the third derivative, are displayed in Table I. One might be disposed to identify this fine structure with the double-peak structure found by Platzman and Eisenberger in early $S(\mathbf{q},\omega)$ measurements on Al, even though the dip position of their measurement was 6 eV at smaller values of energy loss. Nevertheless, these findings have triggered a huge amount of theoretical work, as stated in Sec. I. The physical origin

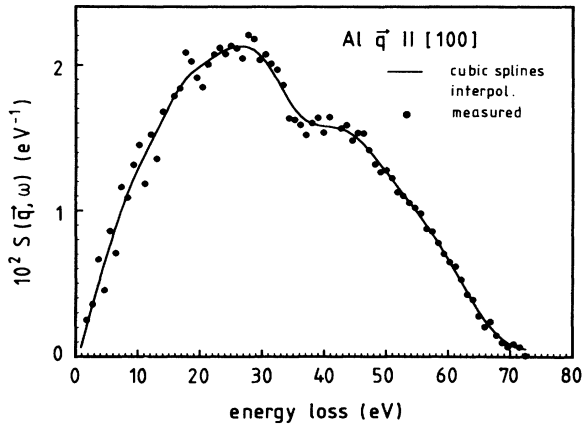

FIG. 1. Full circles: Experimental data of $S(\mathbf{q},\omega)$ of Al for **q** parallel to [100] and $q = 1.45$ a.u., after background subtraction, removal of the quasielastically scattered line, and scaling to absolute values by utilizing the f-sum rule. Solid line: Cubic spline interpolation of the experimental data.

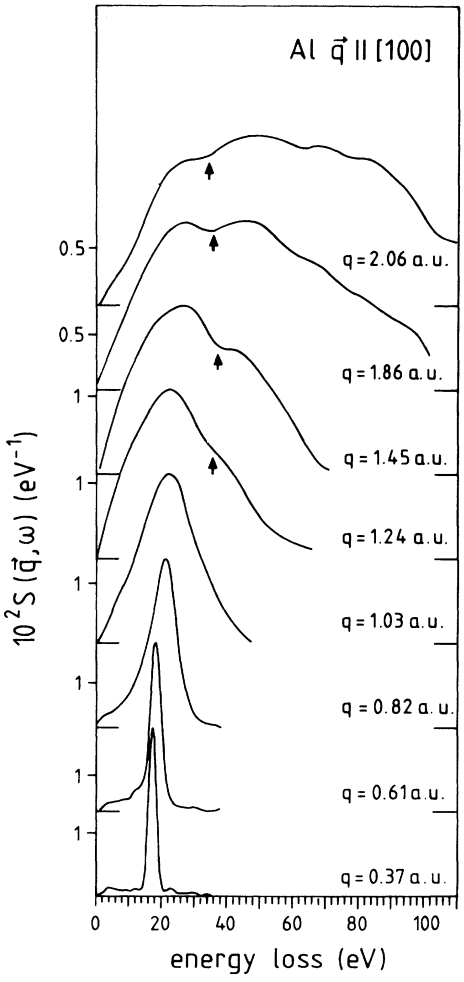

FIG. 2. Cubic-spline-interpolated experimental $S(\mathbf{q},\omega)$ spectra of Al for **q** parallel to [100] and q values as indicated. The arrows mark the position of a local zero of the third derivative, which is attributed in the text to the "dip" position of a **q**-orientation-independent one-peak–one-shoulder or double-peak fine structure.

of this q-orientation-independent fine structure will be discussed in Sec. IV B. Exclusively in the q parallel to [110] spectra, another fine structure can be identified throughout the q range between 0.67 and 1.86 a.u., whose dip position (zero of the third derivative) is marked by full circles in Fig. 3 and tabulated in Table II. It is natural to connect this fine structure with the influence of the g_{220}-Bragg plane on the electron-hole excitation continuum, as will be discussed in Sec. IV B. Further weak fine structure, which is visible for $q > 1.7$ a.u. both in Figs. 2 and 3, might be attributed either the g_{440}-Bragg plane or to the Al L edges, but will not be discussed further.

The most recent synchrotron radiation $S(\mathbf{q},\omega)$ measurements on Al single crystals by Platzman *et al.*[51] are in perfect agreement with our results as far as the overall shape and the dip position of the q-orientation-independent fine structure are concerned. On the contrary, the above authors did not look for q-orientation-dependent fine structure.

B. Comparison with model calculations

It is commonly assumed that the valence electrons of Al behave nearly free-electron-like, at least as far as states near the Fermi energy are concerned. It is therefore near at hand to compare, first of all, the experimental dynamic structure factors of Al with those calculated within the limits of the jellium model, i.e., by using in a first approach $\varepsilon_{SC}(\mathbf{q},\omega)$ of Eq. (4) in Eq. (3) for an "empty lattice," where a small energy width for all one-electron states of 0.03 a.u. has been allowed for. The result of these calculations is equivalent to the jellium-RPA structure factor, as can be obtained by employing Lindhard's well-known dielectric function in analytical form, and is confronted with experiment in Fig. 4(a) for $q = 1.45$ a.u. It is evident, and has already been found for Li (Ref. 7) and Be,[19] that there is a distinct discrepancy between the RPA-peak position, which is at 44 eV, and the experimental peak, found at 29 eV. In a next step, we have used the local-field-corrected $\varepsilon(\mathbf{q},\omega)$ of Eq. (7) in Eq. (3), where the static approximation $G(\mathbf{q})$ of the local-field factor, as calculated by Utsumi and Ichimaru[20] and shown in Fig. 5, has been applied. The result of this calculation, shown together with the experiment in Fig. 4(b), clearly indicates a variation in the right direction, insofar

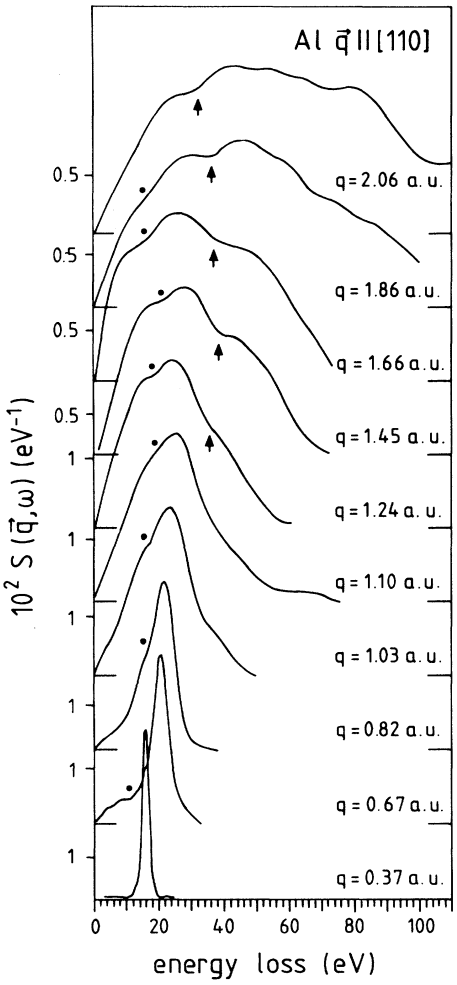

FIG. 3. Cubic-spline-interpolated experimental $S(\mathbf{q},\omega)$ spectra of Al for q parallel to [110] and q values as indicated. The arrows mark the position of a local zero of the third derivative, which is attributed in the text to the "dip" position of a q-orientation-independent one-peak–one-shoulder or double-peak fine structure. Full circles mark the position of another local zero of the third derivative, which is attributed in the text to the "dip" position of a strongly q-orientation-dependent fine structure introduced by a Bragg-reflection-induced indentation in the electron-hole excitation continuum.

TABLE I. Experimental dip position (local zeros of the third derivative) in the Al $S(\mathbf{q},\omega)$ spectra (second column) in relation to both the dip position according to the step model (Ref. 28) for the reciprocal lifetime (third column) and the dip position of the pseudopotential band-structure calculation (fourth column).

		Dip position (eV)		
	q (a.u.)	Expt.	Calc. step model (Ref. 28)	Calc. band structure
q parallel to [100]	1.24	34.7±1.0	29.3	34.6±1.5
	1.45	35.4±1.3	30.1	36.2±1.5
	1.86	34.5±1.6	28.3	36.9±1.5
q parallel to [110]	1.24	35.0±1.0	29.3	35.9±1.5
	1.45	36.9±1.3	30.1	37.8±1.5
	1.86	35.5±1.6	28.3	38.0±1.5

as the peak has now moved to 35 eV and the overall shape of the calculated dynamic structure factor has lost its typical "RPA asymmetry," never found experimentally. In a third step of the approach, we have introduced an energy- (momentum-) dependent lifetime in the sense of an "on-shell approximation" of the self-energy as pointed out in Sec. II. The momentum-dependent inverse lifetime has been calculated by means of a scheme proposed by Quinn and Terrel,[21] and is plotted in Fig. 6. It can be read from Fig. 4(c), where the result of this calculation is presented, that the peak of the calculated struc-

TABLE II. Experimental dip position (local zeros of the third derivative) in the Al $S(\mathbf{q},\omega)$ spectra for $\mathbf{q}$ parallel to [110] (second column) in relation to both the dip position according to Eq. (6) (third column) and the dip position in the pseudopotential band-structure calculations.

	Dip position (eV)		
q (a.u.)	Expt.	Eq. (6)	Band-structure calc.
1.24	18.3±1.0	18.3	18.2±1.0
1.45	20.9±1.5	17.3	19.2±1.0
1.86	14.0±2.0	11.8	11.0±1.0

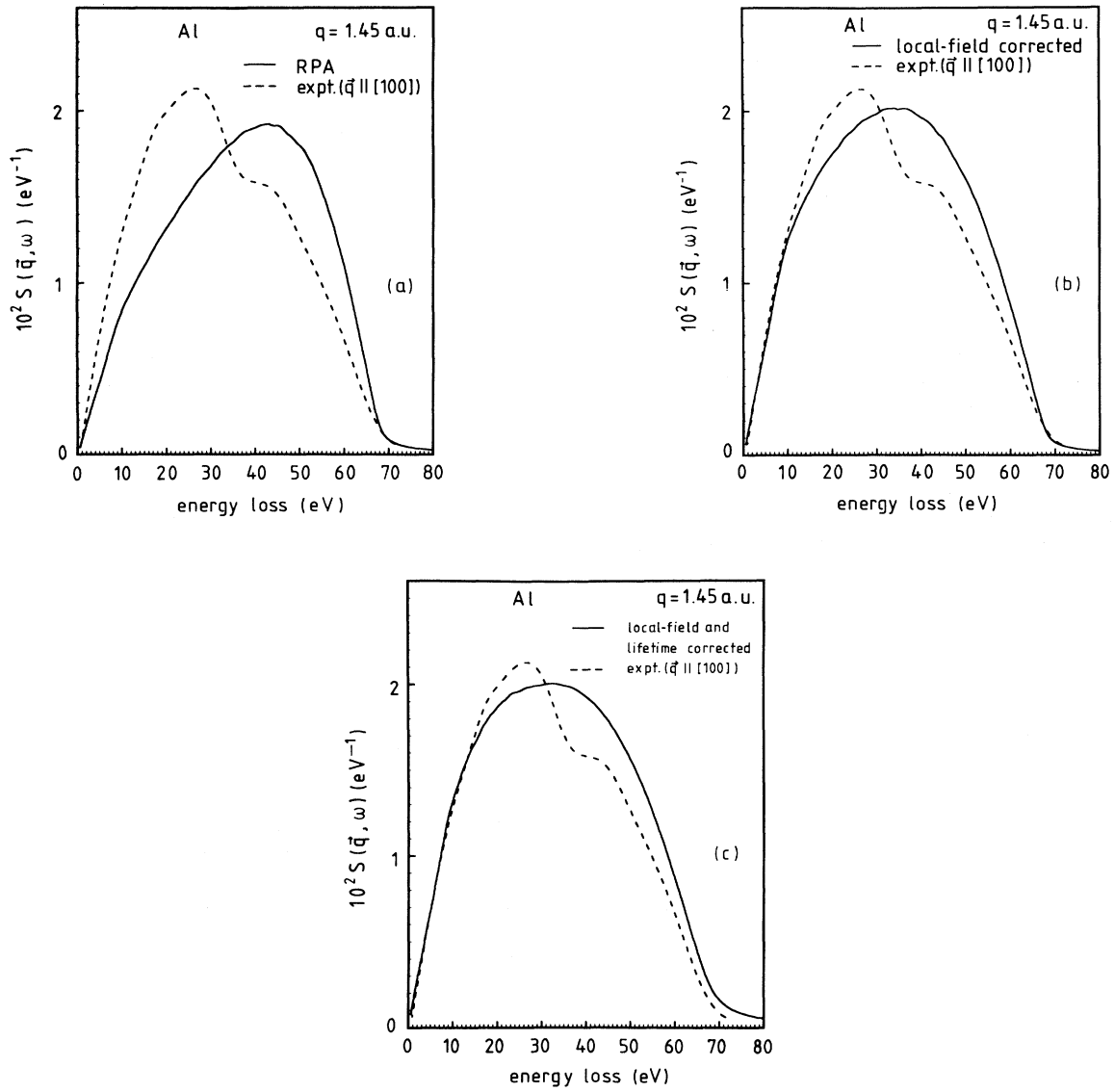

FIG. 4. Experimental $S(\mathbf{q},\omega)$ spectrum (dotted line) of Al for $\mathbf{q}$ parallel to [100] and $q=1.45$ a.u., in relation to a RPA jellium-model-calculated spectrum (solid line). (b) Experimental $S(\mathbf{q},\omega)$ spectrum (dotted line) of Al for $\mathbf{q}$ parallel to [100] and $q=1.45$ a.u., in relation to a jellium-calculated spectrum (solid line), where the RPA result has been local-field corrected according to Eq. (7), and using $G(\mathbf{q})$ of Fig. 5. (c) Experimental $S(\mathbf{q},\omega)$ spectrum (dotted line) of Al for $\mathbf{q}$ parallel to [100] and $q=1.45$ a.u., in relation to a jellium-model-calculated spectrum (solid line), where the RPA result has been local-field and lifetime corrected according to Eqs. (8) and (9), and using $\Gamma(\mathbf{p})$ of Fig. 6.

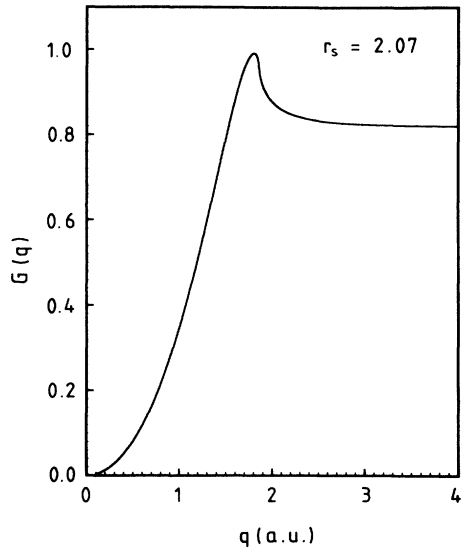

FIG. 5. The static local-field factor $G(\mathbf{q})$ for the electron density of Al metal $r_s=2.07$, according to Ref. 20.

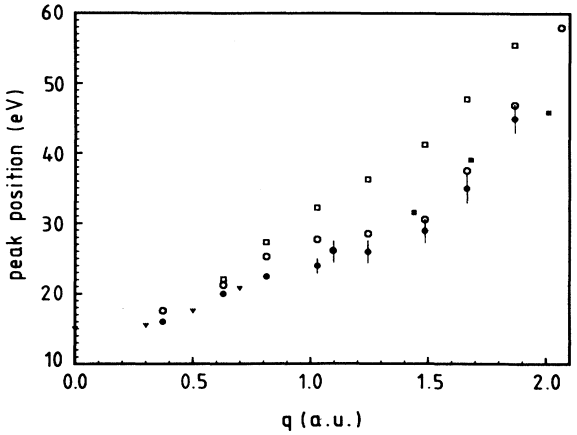

FIG. 7. Peak position of the Al $S(\mathbf{q},\omega)$ spectra as a function of the momentum transfer q. Full circles: IXSS experimental result for $\mathbf{q}$ parallel to [110]. Full triangles: EELS measurements, Ref. 52. Open squares: jellium RPA. Open circles: jellium calculations, local-field and lifetime corrected. Full squares: calculated for $r_s=2$ by Ref. 36 (center-of-gravity extrapolation).

ture factor at 32 eV is now very near the experimental one. In Fig. 7, we have plotted the experimental peak position for $\mathbf{q}$ parallel to [110] as a function of q (full circles), together with the theoretical peak position both according to the RPA (open squares) and the local-field and lifetime-corrected calculation (circles). The result of EELS measurements of Sprösser-Prou[52] for smaller q's are added (triangles). Thus Fig. 7 clearly demonstrates that inclusion of local-field and lifetime corrections leads to a much better agreement between the jellium model and experiment, at least as far as peak positions are concerned.

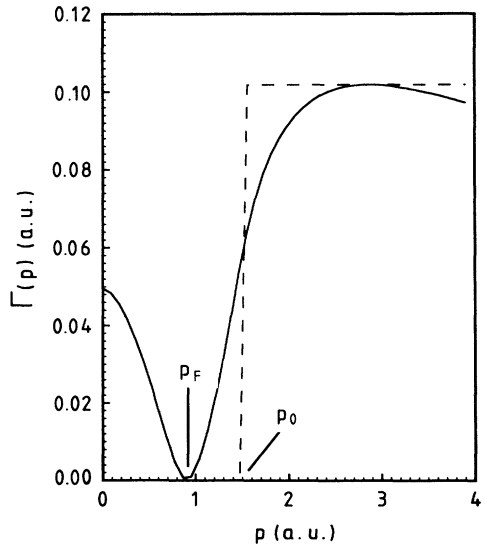

FIG. 6. Solid curve: The inverse momentum-dependent lifetime $\Gamma(\mathbf{p})$ for the electron density of Al metal, according to the scheme of Ref. 21. Dashed line: The step model.

Nevertheless, Fig. 4(c) indicate that approximations within the limits of the jellium model cannot account for the $\mathbf{q}$-orientation-independent fine structure. This is in contrast to the statements of Rahman and Vignale,[28] who have claimed to reproduce this fine structure as a consequence of the steep rise of the reciprocal lifetime for energies large enough to allow for the excitation of a plasmon. Following their scheme, we found a double-peak structure in the calculated $S(\mathbf{q},\omega)$ spectra only when using a simple step model of the reciprocal lifetime as shown in Fig. 6, where p_0 is defined by the following equation:

$$\hbar\omega(q_c)=(p_0^2-\hbar^2k_F^2)/2m, \quad k_F \text{ is the Fermi momentum} . \tag{11}$$

Then one can easily show that a dip in $S(\mathbf{q},\omega)$ will appear at ω_{dip}, given by

$$\hbar\omega_{\text{dip}}=\hbar q(p_0-\hbar q)/2 . \tag{12}$$

We have included the dip positions calculated according to Eq. (12) in Table I. One can see that the experimental dips are off the calculated ones by nearly 5 eV, so that we can rule out the steep rise of the reciprocal lifetime as the origin of the $\mathbf{q}$-orientation-independent dip structure. It has already been mentioned that Ng and Dabrowski[33] have put forward a much more fundamental objection against the application of the "on-shell" approximation of the self-energy, as is characteristic for the lifetime arguments. By making a full "off-shell" calculation of the spectral weight function within the limits of a plasmon-pole model, and by using these spectral weight functions to find $S(\mathbf{q},\omega)$ according to Eq. (10), they have failed to reproduce a fine structure with a dip position as given in Eq. (12). It should be mentioned that Platzman *et al.*[51] have found qualitative agreement of their recent $S(\mathbf{q},\omega)$ measurements on Al with "on-shell" calculations of Mukhopahyay, Kalia, and Singwi,[26] as far as the overall

shape of the $S(\mathbf{q},\omega)$ curves is concerned. But they did not explicitly compare the experimental dip position, which agrees with our findings within experimental error, with the "on-shell"-calculated dip position,[26] which follows Eq. (12) quite well.

Ng and Dabrowski[33] have stressed another point, which seems to us to offer at least a qualitative explanation of the q-orientation-independent double-peak structure, and which is connected with the characteristic structure of the spectral weight function, namely its two strong peaks for $p < k_F$, where this structure has already been found and thoroughly discussed by Lundquist.[39,53] One peak can be identified with the quasiparticle; its dispersion is free-electron-like. The second peak, which has, at least for small p, nearly the same spectral weight as the first one, is situated below the first one by somewhat less than 1.5 times the plasmon energy $\hbar\omega_p$, and can be attributed to a coupled mode of holes and plasmons (plasmaron). The dispersion of this second peak is also nearly quadratic, like the first one, so that their distance is nearly independent of q, but the peak increases in width when approaching k_F, contrary to the behavior of the quasiparticle peak. Looking at Eq. (10), we see that $S(\mathbf{q},\omega)$ is the result of an energy-convoluting double-peaked spectral weight function (at negative energies) with the spectral weight function at positive energies, which is essentially single peaked accompanied by a broad continuum. Thus a double-peak structure of $S(\mathbf{q},\omega)$ is the self-evident consequence of the double-peak structure of $A(\mathbf{p},E)$ for $p < k_F$. Of course, the additional momentum convoluting in Eq. (10) can strongly wash out this double-peak structure. Nevertheless, if the existence of the plasmaron was the origin of the q-orientation-independent fine structure, the distance of its two "peaks" would be equal to the energy distance between the quasiparticle and the plasmaron, which is for Al ($r_s \approx 2$) $1.3\times\hbar\omega_p$ (the weighted average of a RPA calculation[53]). Using the experimental plasmon energy of 14.6 eV at $q=0$ for Al,[52] this energy distance should be 19 eV. In Table III, the position of the "peaks" (zeros of the third derivative) on the right-hand and left-hand side of the q-orientation-independent dip are listed together with their energy distance, which seems not to change systematically with q and exhibits a mean value of 18.1 ± 1.5 eV, consistent with the RPA result. [It has been demonstrated by Petrillo and Sacchetti[54] that local-field correction to the $A(\mathbf{p},E)$ calculations does not significantly change the energy distance between the plasmaron and the quasiparticle for $p < k_F$.] It should be mentioned, and will strengthen this plasmaron-type interpretation of the double-peak fine structure, that a similar more or less q-orientation-independent fine structure in the Li-$S(\mathbf{q},\omega)$ spectra (see Fig. 6 of Ref. 7, especially the q parallel to [111] spectra) exhibits an average "peak" distance of 11 eV, which is not far from $1.45\times\hbar\omega_p$, the weighted average of the RPA calculation of Lundquist[53] for $r_s=3$. To what extent the momentum convolution in Eq. (10) washes out the double-peak structure of the spectral weight function has clearly been shown by Ng and Dabrowski,[33] who have calculated separately the plasmaron-like contribution and the quasiparticle contribution to $S(\mathbf{q},\omega)$. When fitting together both contributions, no significant double-peak structure remains. The only fine structure visible in their spectra can be attributed to rise discontinuities of the various contributions to $S(\mathbf{q},\omega)$, where these discontinuities seem to be due to the plasmon-pole approximation of the dielectric function, which makes both the plasmaron and the quasiparticle peak in $A(\mathbf{p},E)$ for $p < k_f$ δ-function-like. Therefore, we can state that it is rather unlikely that the double-peak structure of the measured $S(\mathbf{q},\omega)$ spectra is a direct consequence of the plasmaron-quasiparticle doublet of the spectral weight function, even though the very similar energy distance of both double-peak structures and the q independence of this energy distance in the experimental spectra is rather striking.

As already mentioned in the Introduction, Green, Neilson, and Szymanski[36] have found some fine structure in their calculations of $S(\mathbf{q},\omega)$ by utilizing fully conserving diagrammatic perturbation methods, which could be attributed to multiple-pair excitations. Comparing their $r_s=2$ calculation with our experimental results at similar q values, no assignment of fine structures could be found. But the extrapolated centers of gravity of their calculated $S(\mathbf{q},\omega)$ spectra are inserted into Fig. 7 (full squares), indicating a quite reasonable agreement with experiment, as already found in Ref. 36, when the calculations were compared with the experimental results of Priftis, Boviatsis, and Vradis.[24]

It has already been pointed out in Ref. 19 that even a nearly q-orientation-independent fine structure could be originated by band-structure effects. This possibility will be discussed in what follows. Whenever the q-orientation-independent dip in our results should be due to band structure, then the very weak dispersion of its dip position, as given in Table I, supports the assumption that this fine structure must correspond to a strong deviation from free-electron-like behavior of the unoccupied states. Looking for indications of strong deviations from free-electron-like behavior of unoccupied states in other spectroscopies, we found that the K-absorption spectra[55] as well as the L-absorption spectra[56] of Al exhibit a distinct diplike deviation from free-electron-like behavior between 27 and 30 eV above threshold. This diplike structure has been found in high-energy band-structure calculations of the density of states (DOS) performed by Connolly[57] and Ojala,[58] is most pronounced in the partial

TABLE III. Experimental position of the adjacent zeros of the third derivative ("peaks") on the low- (second column) and high-energy (third column) sides of the q-orientation-independent dip in the q parallel to [100] Al $S(\mathbf{q},\omega)$ spectra. In the fourth column, the energy difference between these "peak" positions are tabulated.

q (a.u.)	"Peak" position (eV) low	high	Energy distance (eV)
1.24	21.7±1.0	40.0±1.0	18.3±2.0
1.45	26.3±1.5	43.6±1.0	17.3±3.0
1.86	26.0±1.5	45.0±1.0	19.0±3.0
2.06	25.0±2.0	43.0±1.0	18.0±4.0

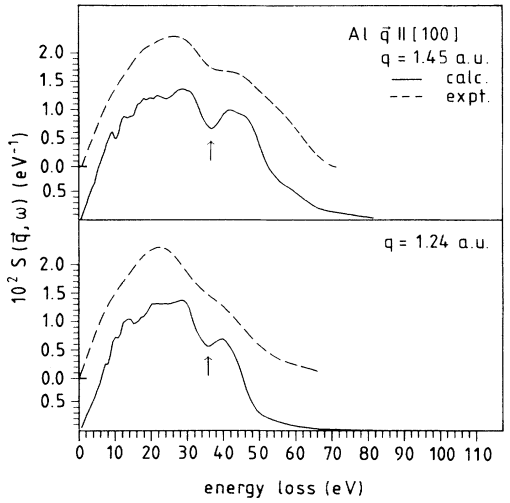

FIG. 8. Experimental Al $S(\mathbf{q},\omega)$ spectra (dotted line) for $\mathbf{q}$ parallel to [100] in relation to pseudopotential band-structure-calculated ones (solid lines) obtained by using potential coefficients of Ref. 57, and by including local-field and lifetime corrections. Arrows indicate dip positions due to the downshift of d-like bands.

DOS of the d-like states, and has been attributed to a shift to lower energies of the more localized unoccupied states with prominent d symmetry (mainly X_5, X_2, $W_{1'}$) due to the lack of d-core states in Al, to which the valence states have to be orthogonalized. This shift leads to a narrowing of the corresponding d-like band. Such a prominent structure of the DOS should leave behind some structure in $S(\mathbf{q},\omega)$ which can be expected to be nearly $\mathbf{q}$ orientation independent, since the relevant states are more or less isotropically distributed in the $\mathbf{k}$ space. Moreover, the dispersion of this structure, $\hbar\omega_s(q)$, should follow roughly Eq. (6), where $g/2$ has to be substituted with k_s, the average length of vectors of the extended k space, which belong to the lowered d-like states. Connally[57] has fitted pseudopotential coefficients ranging from V_{111} to V_{511} to his augmented plane wave (APW) calculations in order to reproduce this d-band narrowing within the limits of a local pseudopotential scheme. We have made use of these coefficients and have performed a self-consistent field calculation of $S(\mathbf{q},\omega)$ for $\mathbf{q}$ parallel to [100] and $\mathbf{q}$ parallel to [110], respectively, according to Eq. (4), including, as in the case of the jellium calculations, both the local-field corrections following Eq. (7) and the momentum-dependent lifetime [see Eqs. (8) and (9)]. The results of these calculations are shown in Figs. 8 and 9, together with the corresponding experimental result. For both $\mathbf{q}$ orientations, one can clearly see the dip around 36 eV due to the narrowing of the d-like bands. Figure 10 demonstrates exemplarily the downshift of the X_5, X_2, and $W_{1'}$ states, together with the resulting energy

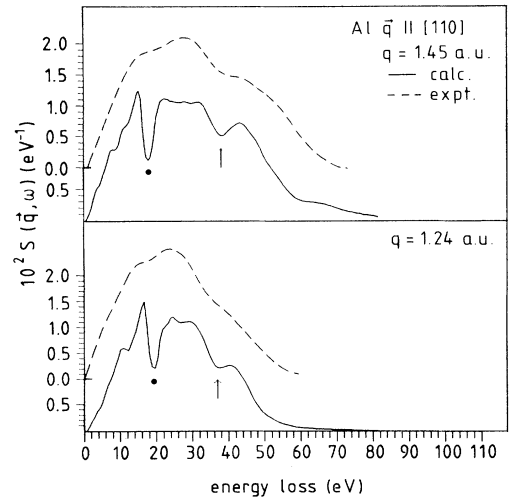

FIG. 9. Experimental Al $S(\mathbf{q},\omega)$ spectra (dotted line) for $\mathbf{q}$ parallel to [100] in relation to pseudopotential band-structure-calculated ones (solid line) obtained as in Fig. 8. Arrows indicate the dip position due to the downshift of d-like bands. Full points indicate dip positions due to the g_{220}-Bragg-plane-induced excitation gap.

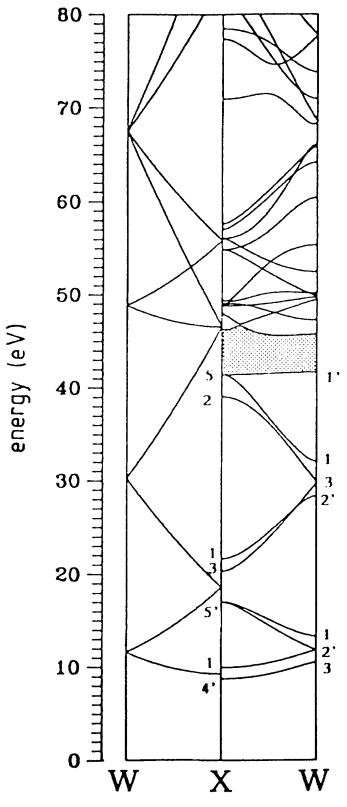

FIG. 10. Right-hand side: the pseudopotential band structure of Al in the X-W direction using pseudopotential coefficients and notation for the representations of Ref. 57. The downshift of the d-like states (X_5,X_2,W_1') with respect to the empty-lattice band structure on the left-hand side, together with the resulting energy gap, are indicated by screening. Left-hand side: the empty-lattice band structure of Al in the X-W direction.

gap (screened), by comparing our pseudopotential band-structure calculations with the empty-lattice band structure. The ripples for energies below 20 eV found in our calculations are due to the coarse **k**-space sampling and to a lifetime broadening less than above 20 eV. The calculated dip positions are compared with the experimental ones in Table I, and agree within experimental and calculation error limits. Of course, the experimental dips are much less pronounced than the calculated ones. We attribute this lower contrast in the experiment to the influence of continuum states above the Fermi level, which should accompany the quasiparticle states, according to calculations first done by Lundquist.[39] It might be worthwhile to mention that also in the case of Li,[7] where we have found a very similar **q**-orientation-independent fine structure, a strong dip is found in the DOS (Ref. 59) roughly 14 eV apart from the Fermi level, so that the dip position in $S(\mathbf{q},\omega)$ should be visible around 16 eV, just where we have found it experimentally. It should be mentioned, as it would give support to our interpretation, that, in the case of Li, it is a *p*-band narrowing which is responsible for the dip in the DOS, and which can be traced back to the lack of core *p* states.

An additional very strong dip is seen in the calculated $S(\mathbf{q},\omega)$ spectra for **q** parallel to [110] of Fig. 9, whose position is entered in Table II and coincides nicely with the experimental **q**-orientation-dependent dip position in this table, where this dip has been attributed to the influence of the $\mathbf{g}_{220}$-Bragg plane on the electron-hole continuum, as discussed in Sec. II in connection with Eq. (6). Of course, the calculated dip is much more pronounced than the experimental one. This might be due to the band order along the $X\Gamma$ direction obtained in the pseudopotential calculation, which opens a large excitation gap and which does not fit the APW calculation of Connolly[57] in this respect. Nevertheless, it seems that the band-calculated dip position better fits the experiment than that calculated according to the simple kinematical Eq. (6).

V. CONCLUSIONS

The comparison of the experimental dynamic structure factor $S(\mathbf{q},\omega)$ of single crystals of Al with various theoretical models has led to the following conclusions.

(i) As already stated for other simple metals, and also in the case of Al, the RPA cannot describe appropriately the gross features of the short-range correlation of electrons as measured with the dynamic structure factor for larger q's ($q > q_c$).

(ii) Only by taking into account local-field corrections together with multiexcitations (lifetime effects and/or multiple-pair excitation) can the short-range electron correlation be considered appropriately in such a manner that the overall features of $S(\mathbf{q},\omega)$ are correctly represented.

(iii) The **q**-orientation-dependent fine structure of the $S(\mathbf{q},\omega)$ spectra can be attributed to ion-lattice-induced indentations in the electron-hole excitation continuum due to Bragg reflection.

(iv) The problem of the **q**-orientation-independent double-peak or one-peak–one-shoulder fine structure of $S(\mathbf{q},\omega)$ could not be solved definitely, even though it seems to be most reasonable to consider this fine structure to be a consequence of the narrowing of unoccupied *d*-like bands, due to the lack of *d*-core states. Only this band-structure-based model could offer a semiquantitative agreement with experiment. All other models for interpreting this fine structure on the basis of special features of correlation-induced excitations have either failed or could deliver only rather speculative qualitative arguments, so that they need further experimental and theoretical verification in order to take them seriously into consideration.

ACKNOWLEDGMENT

This work has been funded by the German Federal Ministry of Research and Technology under Contract No. 05-434 AXB.

[1]N. D. Mermin, Phys. Rev. B **1**, 2362 (1970).
[2]K. L. Kliewer and H. Raether, Phys. Rev. Lett. **30**, 971 (1973).
[3]H. Raether, *Springer Tracts in Modern Physics* (Springer, Berlin, 1980), Vol. 88.
[4]J. Fink, in *Unoccupied Electronic States,* edited by J. C. Fuggle and J. E. Inglesfield, Topics in Applied Physics Vol. 69 (Springer, Berlin, 1992).
[5]P. Eisenberger, P. M. Platzman, and K. C. Pandy, Phys. Rev. Lett. **31**, 311 (1973).
[6]P. Eisenberger, P. M. Platzman, and P. Schmidt, Phys. Rev. Lett. **34**, 18 (1975).
[7]W. Schülke, H. Nagasawa, S. Mourikis, and P. Lanzki, Phys. Rev. B **33**, 6744 (1986).
[8]K. Sturm, Adv. Phys. **31**, 1 (1982).
[9]W. M. Saslow and G. F. Reiter, Phys. Rev. B **7**, 2995 (1973).
[10]A. vom Feld, J. Sprösser-Prou, and J. Fink, Phys. Rev. B **40**, 10 181 (1989).
[11]K. Sturm, Solid State Commun. **48**, 29 (1983).
[12]K. Sturm, E. Zaremba, and K. Nuroh, Phys. Rev. B **42**, 6973 (1990).
[13]E.-Ni Foo and J. J. Hopfield, Phys. Rev. **173**, 635 (1968).
[14]K. Sturm and L. E. Oliveira, Phys. Rev. B **30**, 4351 (1984).
[15]C. H. Chen and J. Silcox, Phys. Rev. B **16**, 4246 (1977).
[16]W. Schülke, H. Nagasawa, and S. Mourikis, Phys. Rev. Lett. **52**, 2065 (1984).
[17]W. Schülke, U. Bonse, H. Nagasawa, S. Mourikis, and A. Kaprolat, Phys. Rev. Lett. **59**, 1362 (1987).
[18]E. Burkel, *Springer Tracts in Modern Physics* (Springer, Berlin, 1991), Vol. 125.
[19]W. Schülke, H. Nagasawa, S. Mourikis, and A. Kaprolat, Phys. Rev. B **40**, 12 215 (1989).
[20]K. Utsumi and S. Ichimaru, Phys. Rev. B **22**, 1522 (1980); **22**, 5203 (1980); **23**, 3291 (1981).
[21]J. J. Quinn and R. A. Terrell, Phys. Rev. **112**, 812 (1958).
[22]R. J. Shaw, J. Phys. C **2**, 2350 (1969).
[23]W. Schülke and W. Lautner, Phys. Status Solidi B **66**, 211 (1974).
[24]G. D. Priftis, J. Boviatsis, and A. Vradis, Phys. Lett. **68A**, 482 (1978).
[25]P. M. Platzman and P. Eisenberger, Phys. Rev. Lett. **33**, 152

(1974).
[26]G. Mukhopadhyay, R. K. Kalia, and K. S. Singwi, Phys. Rev. Lett. **15**, 950 (1975).
[27]K. Awa, H. Yasuhara, and T. Asahi, Phys. Rev. B **25**, 3670 (1982); **25**, 3687 (1982).
[28]S. Rahman and G. Vignale, Phys. Rev. B **30**, 6951 (1984).
[29]G. Mukhopadhyay and A. Sjölander, Phys. Rev. B **17**, 3589 (1978).
[30]G. Niklasson, A. Sjölander, and F. Yoshida, J. Phys. Soc. Jpn. **52**, 2140 (1983).
[31]F. Green, D. Neilson, and J. Szymanski, Phys. Rev. B **31**, 2796 (1985).
[32]G. Niklasson, Solid State Commun. **54**, 665 (1985).
[33]T. K. Ng and B. Dabrowski, Phys. Rev. B **33**, 5358 (1986).
[34]F. Green, D. Neilson, and J. Szymanski, Phys. Rev. B **35**, 124 (1987).
[35]E. Pajanne, J. Phys. C **15**, 5629 (1982).
[36]F. Green, D. Neilson, and J. Szymanski, Phys. Rev. B **31**, 2779 (1985); **31**, 5837 (1985).
[37]G. Baym and L. P. Kadanoff, Phys. Rev. **124**, 287 (1961).
[38]F. Green, D. Neilson, D. Pines, and J. Szymanski, Phys. Rev. B **35**, 133 (1987).
[39]B. I. Lundquist, Phys. Kondens. Mater. **6**, 193 (1967); **6**, 206 (1967).
[40]P. Noziéres and D. Pines, Phys. Rev. **113**, 1254 (1959).
[41]D. Pines and P. Noziéres, *The Theory of Quantum Liquids* (Benjamin, New York, 1966), Vol. 1.
[42]H. Ehrenreich, and M. H. Cohen, Phys. Rev. **115**, 786 (1959).
[43]J. Hubbard, Proc. R. Soc. London Ser. A **243**, 336 (1957).
[44]W. Schülke and H. Nagasawa, Nucl. Instrum. Methods **222**, 203 (1984).
[45]W. Schülke, Nucl. Instrum. Methods A **246**, 491 (1986).
[46]A. Berthold, S. Mourikis, J. R. Schmitz, W. Schülke, and H. Schulte-Schrepping, Nucl. Instrum. Methods A **317**, 373 (1992).
[47]C. J. Sparks, G. E. Ice, J. Wong, and B. W. Batterman, Nucl. Instrum. Methods **172**, 237 (1980).
[48]W. Schülke, in *Handbook on Synchrotron Radiation,* edited by G. Brown and D. E. Moncton (North-Holland, Amsterdam, 1991), pp. 565–637.
[49]C. Reinsch, Numer. Mathematik **10**, 177 (1967); **16**, 451 (1971).
[50]P. C. Gibbons, S. E. Schnatterly, J. J. Ritsko, and J. R. Fields, Phys. Rev. B **13**, 2451 (1976).
[51]P. M. Platzman, E. D. Isaacs, H. Williams, P. Zschak, and G. E. Ice, Phys. Rev. B **46**, 12 943 (1992).
[52]J. Sprösser-Prou, A. von Felde, and J. Fink, Phys. Rev. B **40**, 5799 (1989).
[53]B. I. Lundquist, Phys. Kondens. Mater. **7**, 117 (1968).
[54]C. Petrillo and F. Sacchetti, Phys. Rev. B **38**, 3834 (1988).
[55]C. Senemaud and M. T. Costa Lima, J. Phys. Chem. Solids **37**, 83 (1976).
[56]R. Haensel, G. Keitel, B. Sonntag, C. Kunz, and P. Schreiber, Phys. Status Solidi A **2**, 85 (1970).
[57]J. W. D. Connolly, Int. J. Quantum Chem. **35**, 807 (1970).
[58]E. Ojala, Phys. Status Solidi B **119**, 269 (1983).
[59]D. A. Papcontantopoulos, *Handbook of the Band Structure of Elemental Solids* (Plenum, New York, 1986), p. 34.